COMMUNICATION

Augmenting Metallobasicity to Modulate Gold Hydrogen Bonding

Logan T. Maltz, Lewis C. Wilkins, and François P. Gabbaï *

6Received 00th January 20xx,
Accepted 00th January 20xx

DOI: 10.1039/x0xx00000x

We report the synthesis and characterization of two phosphine gold carbinol species exhibiting intramolecular Au···H-O hydrogen bonding. Increasing the metallobasicity of gold through chloride to phenyl ligand substitution produced an observable increase in this hydrogen bond's strength which was analyzed experimentally and computationally.

Despite its ubiquity, the hydrogen bond (HB) is actually an ambiguously-defined concept that some date back to 1920, if not earlier.[1, 2] In 2011, the International Union of Pure and Applied Chemistry (IUPAC) commissioned a committee of researchers to develop an authoritative definition of the HB.[3] Drawing on almost 100 years of examples, this committee concluded that an HB is simply an "attractive interaction" between protic hydrogen and an acceptor with "evidence of bond formation."[3] As a part of this definition, the committee clarified that HBs involve more than just electrostatic interactions—charge transfer and dispersion interactions also provide substantial contributions.[3] One particularly interesting example described in the committee's supporting background information is hydrogen bonding involving transition metals as HB acceptors.[2]

The early 1960s saw the suggestion that transition metals could act as HB acceptors, but it was not until around the 1990s that this bonding motif gained more attention.[4] These HB interactions are distinct from agostic interactions because they involve a filled as opposed to an empty metal orbital, producing a 3c-4e interaction instead of the 3c-2e interaction seen for agostic species (Figure 1).[1] Obvious HB acceptor candidates were late transition metals as these metals are more electron rich and more electronegative than the early metals.

Platinum(II) examples have been particularly well represented because this d^8, relatively electronegative metal adopts a square-planar geometry with a filled dz^2-orbital poised to engage the σ*-orbital of an HB donor.[4, 5] Platinum's prevalence in this chemistry is partly due to relativistic effects which not only enhance its electronegativity but also increase its metallobasicity by making its d-orbitals more diffuse.[6] Perhaps most surprising is the strength of these interactions: in 2014, Baya *et al.* used Atoms in Molecules (AIM) analysis to estimate the strength of the Pt^{II}···H-O interaction in **A** to be 8-10 kcal mol^{-1} (Figure 1).[7]

Neighboring platinum in the periodic table, gold seems like an ideal candidate for an HB acceptor. Because of accentuated relativistic effects, gold displays an anomalously large electron affinity and ionization energy.[6] These atomic properties are directly correlated to this element's high electronegativity, which—as explained by Berger, Schoiber, and Monkowius—sets the stage for its involvement in hydrogen bonding.[8] The linearity of d^{10} Au(I) complexes also facilitates approach of the HB donor group as supported by early evidence from Schmidbaur *et al.*[9] Since then, several computational papers[10, 11]—including from the Esterhuysen group[12-14]—have been published, indicating that Au(I) should indeed engage in hydrogen bonding.

Two 2019 papers—one by Straka *et al.* (**B**) and the other by Rigoulet *et al.* (**C**)—provided the first experimental evidence for intramolecular Au···H-N^+ hydrogen bonding (Figure 1).[15, 16] Both papers took advantage of a cationic ammonium species

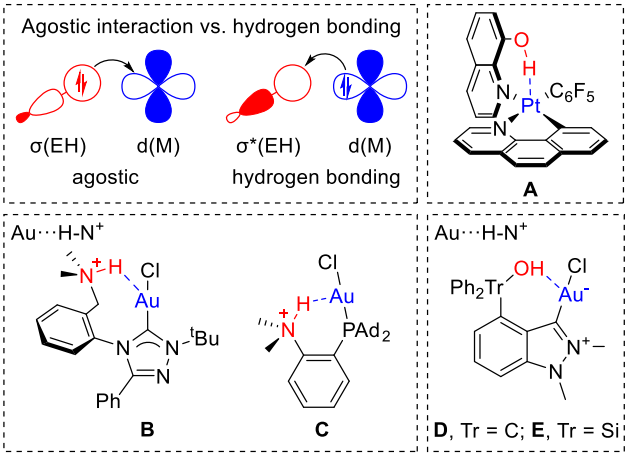

Fig. 1 Top left: Agostic interaction vs. hydrogen bonding. Top right: Example of Pt···H-O HB.[7] Bottom: Examples of experimentally validated Au···H-N^+ and Au···H-O HBs.[15-17]

Department of Chemistry, Texas A&M University, College Station, TX 77843, USA. Email: francois@tamu.edu

† Electronic supplementary information (ESI) available: Additional experimental and computational details and crystallographic data in cif format. CCDC 2178883-2178885 and 2191898. For ESI and crystallographic data in CIF or other electronic format see DOI: 10.1039/x0xx00000x.

COMMUNICATION

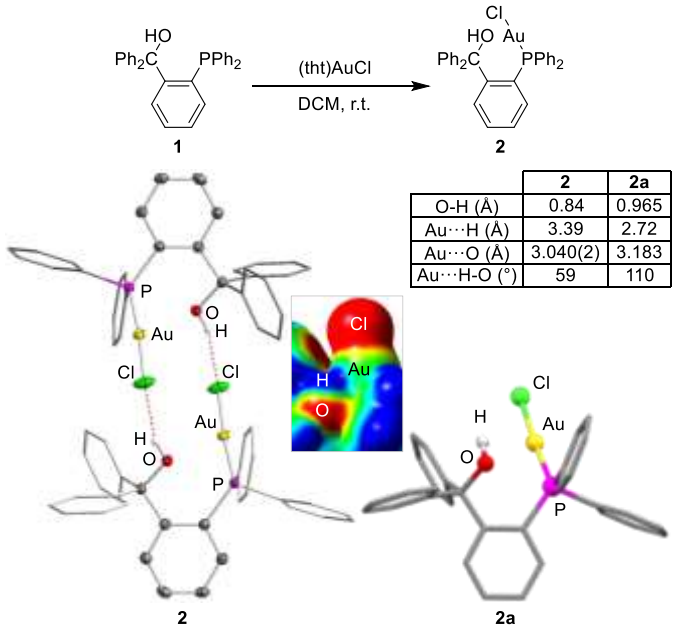

	2	2a
O-H (Å)	0.84	0.965
Au···H (Å)	3.39	2.72
Au···O (Å)	3.040(2)	3.183
Au···H-O (°)	59	110

Fig. 2 Top: Reaction scheme for synthesis of **2**. Bottom: Crystal structure of **2** and its optimized monomer geometry (**2a**). Hydrogens other than O*H* omitted for clarity. Thermal ellipsoids drawn at 50% probability, and phenyl groups drawn as thin lines. Inset shows cropped ESP map for **2a** (color scale: red, -0.04 au; blue, 0.025 au; surface isovalue of 0.005 au). The metrical parameters involving the HB are based on those calculated using the hydrogen atom refinement riding model.

adjacent to the gold center to promote this interaction. Neutral hydroxyl species—with decreased acidity of the HB donor—are inherently more elusive as noted in prior contributions.[9, 10, 12] Against this backdrop, our group reported experimental evidence for intramolecular Au···H-O hydrogen bonding with a carbene-anchored gold center adjacent to either a triaryl carbinol (**D**) or a triaryl silanol (**E**) (Figure 1).[17] With the legitimacy of gold hydrogen bonding experimentally validated, our lab turned its attention to further investigating this unique interaction.

Comparing the Au···H-O HB in **D** with the Au···H-N$^+$ HB in **B**, increased acidity produces a marked increase in the interaction energy.[15, 17] Sophomore organic chemistry lends us plenty of ideas for how one might increase the acidity of a hydroxyl functionality; however, modulating the basicity of a metal center is not as well understood. Through their computational investigations of simple gold *N*-heterocyclic carbene complexes, the Esterhuysen group has suggested that electron-releasing co-ligands increase the electron density at gold, thus strengthening Au···H-X interactions (X = N, O, F).[12, 14] Until now, co-ligand substitution for increasing HB strength has remained synthetically unexplored.

Drawing on our previous synthetic knowledge and taking advantage of the simplicity of phosphine coordination to metals, we combined **1**[18] with (tht)AuCl (tht = tetrahydrothiophene) in dichloromethane at room temperature to synthesize **2**. This compound's synthesis was accompanied by a significant downfield shift in the ^{31}P NMR spectrum from -15.99 ppm to 35.74 ppm. Layering of diethyl ether over the reaction solution yielded colorless block crystals, and single-crystal X-ray diffraction (SCXRD) further verified the identity of the compound (Figure 2). **2** makes a dimer in the solid state, forming classical HBs between the chloride and the carbinol with close Cl···H contacts of 2.36 Å, short Cl···O distances of 3.16 Å, and almost linear Cl···H-O angles of 158°. This classical hydrogen bonding was also confirmed via IR analysis with the OH stretching frequency appearing at a low energy of 3,420 cm^{-1} (ν_{OD} = 2,540 cm^{-1}).[19] Our story has an HB, but it seems to be missing gold.

Despite this apparent setback, the solution-state ^{1}H NMR spectrum piqued our interest. The chemical shift for the hydroxyl proton was seen at 3.08 ppm, downfield of the 2.79 ppm chemical shift seen for triphenylmethanol in $CDCl_3$.[20] While deshielding of the proton can be indicative of an HB, other data is necessary to corroborate this assignment.[3]

Recognizing that the classical intermolecular Cl···H-O HB in the solid state might have been preventing observation of the weaker Au···H-O HB, we turned to gas-phase calculations to assess the possible existence of an HB in the monomer of **2**. Using the mPW1PW91 functional with a mixed basis set (Au cc-pVTZ-PP; P/Cl 6-31G(d',p'); H/C/O 6-31G(d,p)), we optimized the structure of monomeric **2** starting from the SCXRD coordinates to obtain **2a** (Figure 2). The most prominent difference between **2** and **2a** was the OH bond pointing toward the gold center in **2a**. Furthermore, at 2.72 Å, the Au···H

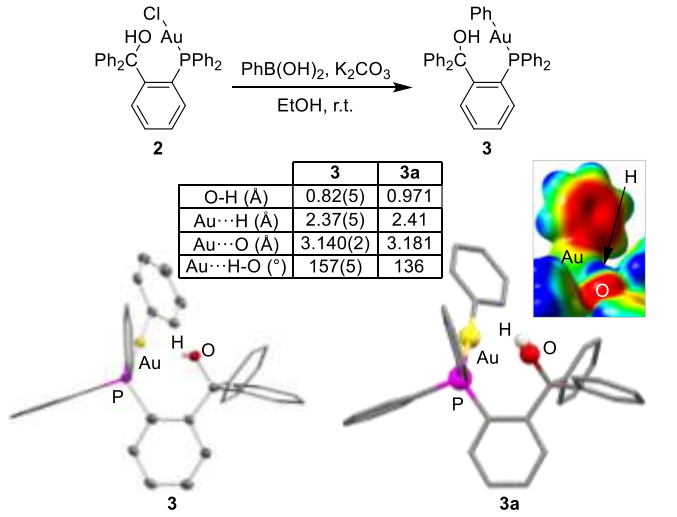

	3	3a
O-H (Å)	0.82(5)	0.971
Au···H (Å)	2.37(5)	2.41
Au···O (Å)	3.140(2)	3.181
Au···H-O (°)	157(5)	136

Fig. 3 Top: Reaction scheme for synthesis of **3**. Bottom: Crystal structure of **3** and its optimized geometry (**3a**). Hydrogens other than O*H* omitted for clarity. Thermal ellipsoids drawn at 50% probability, and phenyl groups drawn as thin lines. Inset shows cropped ESP map for **3a** (color scale: red, -0.04 au; blue, 0.025 au; surface isovalue of 0.005 au).

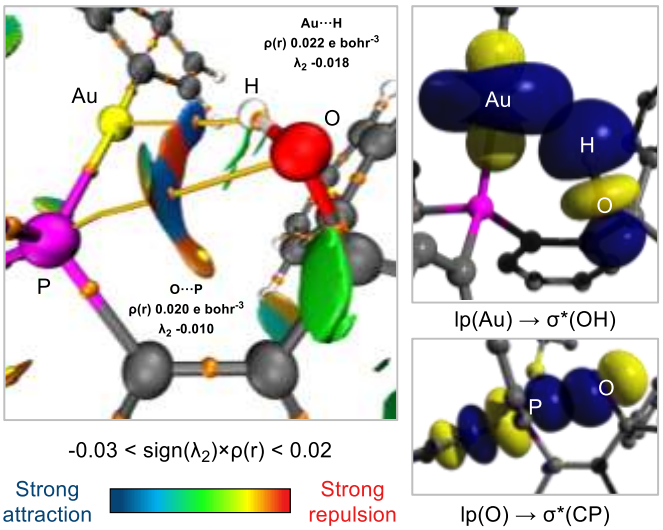

Fig. 4 Left: AIM/NCI plot of **3a** with gradient isosurface of 0.3 au. Right: Selected NBOs for lp(Au) → σ*(OH) and lp(O) → σ*(CP) interactions in **3a**.

distance was just inside the sum of the van der Waals radii (2.86 Å), and the Au···H-O angle was 110°.[21] We probed this interaction using natural bond orbital (NBO) calculations, revealing a lp(Au) → σ*(OH) interaction with a second-order perturbation energy of E(2) = 1.48 kcal mol^{-1}. Despite these promising metrics, AIM analysis did not detect a bond path between the carbinol and gold. Considering this information as a whole, if **2a** exhibits an Au···H-O HB, it is rather weak. We now had a computationally validated—albeit weak—Au···H-O HB, but we wanted to augment this interaction by increasing the metallobasicity of Au to obtain an experimentally verifiable Au···H-O HB.

Inspired by a 2020 report from Tzouras *et al.*, we were confident we could substitute phenyl for chloride under mild conditions.[22] This exchange would not only remove a competing HB acceptor but also donate more electron density to the gold center, thereby increasing the center's metallobasicity. Gratifyingly, we effected this conversion with ^{31}P NMR indicating a mostly clean shift from **2** at 35.74 ppm to **3** at 48.43 ppm. This successful synthesis was further confirmed via SCXRD (Figure 3). Unlike **2**, the crystal structure of **3** depicts the OH facing the gold center. With an Au···H distance of 2.37(5) Å and an Au···O distance of 3.140(2) Å, the HB is within the sum of the van der Waals radii (2.86 Å and 3.18 Å, respectively).[21] Furthermore, there is a much more linear Au···H-O angle of 157(5)°. Two other polymorphs of **3** were isolated (Figure S9). One polymorph contained interstitial solvent which seemed to weaken the HB interaction (Au···H: 2.72(4) Å, Au···O: 3.264(3) Å, Au···H-O: 133(4)°). The other polymorph exhibited an Au···H distance of 3.21(4) Å, an Au···O distance of 3.173(2) Å, and an Au···H-O angle of 81(3)°, signaling the loss of the Au···H-O HB and physically illustrating the weak nature of this noncovalent interaction.

Even so, spectral data supported the strengthening of the HB in going from **2** to **3**. ^{1}H NMR revealed a downfield shift from 3.01 ppm to 3.86 ppm for the hydroxyl proton. Furthermore, with an O-H stretch at 3,570 cm^{-1} (ν_{OD} = 2,610 cm^{-1}), **3** lies within the range of other hydrogen bonded species.[19]

With the inherent difficulty in pinpointing a proton's location next to such a heavy element as gold and with the desire to compare the phenylated system to the chlorinated one, we performed a gas-phase optimization of **3**, producing **3a** (Figure 3).[23] Comparing **2a** to **3a**, we immediately saw favorable metrics indicating an increase in the strength of the HB. **3a** had a significant 0.31 Å decrease in the Au···H distance with respect to **2a** (2.41 Å vs. 2.72 Å). There was also a concomitant decrease in the Au···O distance, an increase in the O-H bond length, and an increased linearization of the Au···H-O angle by 26°. Furthermore, the second-order perturbation energy for the similar lp(Au) → σ*(OH) interaction increased by 3.09 kcal mol^{-1} to E(2) = 4.57 kcal mol^{-1}. Other Au lp-orbitals—not seen in **2a**—donated to the σ*(OH)-orbital in **3a**, ultimately providing a total deletion energy of E_{del} = 8.78 kcal mol^{-1}.

While NBO calculations speak to the charge transfer component of the HB, the ESP maps of **2a** and **3a** in Figures 2 and 3 clearly indicate the electrostatic nature of the interaction. Beyond visualizing the protic nature of the acidic hydrogen, the increased basicity of the gold can be seen by the shifting of electron density from the ligand to the metal center. This shift was corroborated by the decrease in the natural population analysis (NPA) charge on Au from 0.31 in **2a** to 0.23 in **3a**.

To further understand the nature of the HB in **3**, we undertook deeper computational analyses. Unlike the case of **2a**, AIM analysis revealed a bond path in **3a** connecting Au and H. With an electron density $\rho(r)$ of 0.022 e bohr^{-3} at the bond critical point, this HB falls within the range of other HB interactions and is estimated to have an overall interaction energy of about 4 kcal mol^{-1}.[24] The positive Laplacian $\nabla^2\rho(r)$ (0.056 e bohr^{-5}) and negative second Hessian eigenvalue λ_2 (-0.018) further evinced the bonding nature of this noncovalent interaction.[7, 16] The Noncovalent Interaction (NCI) plot in Figure 4 visualizes the strong attraction seen for this Au···H-O HB with the large negative value of sign(λ_2)×$\rho(r)$ depicted as a dark blue. Of course, an equally strong interaction with similar metrics is seen for the lp(O) → σ*(CP) interaction. This interaction was also seen via NBO analysis with both oxygen lone pairs interacting with the C-P σ*-orbital for a total deletion energy of E_{del} = 5.40 kcal mol^{-1}. We contend that this interaction—also seen in **2a**—promotes the HB in these systems by acidifying the proton.

As highlighted by Park *et al.* and Groenewald *et al.*, relativistic effects play a significant role in gold's metallobasicity and therefore its participation in hydrogen bonding.[8, 13, 17] Reoptimizing **3** using the non-relativistic basis set cc-pVTZ-PP-

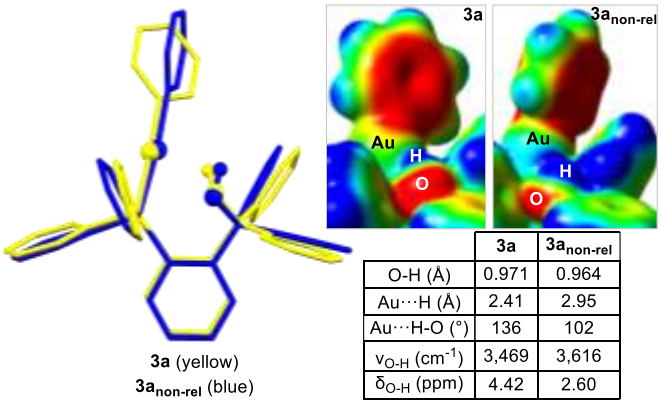

	3a	3a$_{non-rel}$
O-H (Å)	0.971	0.964
Au···H (Å)	2.41	2.95
Au···H-O (°)	136	102
ν_{O-H} (cm^{-1})	3,469	3,616
δ_{O-H} (ppm)	4.42	2.60

Fig. 5 Left: Structure overlay for **3a**/**3a**$_{non-rel}$. Right top: The insets show cropped ESP maps for **3a** and **3a**$_{non-rel}$ (color scale: red, -0.04 au; blue, 0.025 au; surface isovalue of 0.005 au). Right bottom: Table providing selected computational structural and spectral data.

NR with the ECP60 MHF pseudopotential for gold, we obtained **3a$_{non-rel}$** which exhibited no hydrogen bonding. The Au···H distance increased to 2.95 Å, the NBO interactions from lp(Au) → σ*(OH) were minimal, and the Au···H bond path seen in the AIM analysis for **3a** disappeared for **3a$_{non-rel}$**. The ESP map of **3a$_{non-rel}$** in Figure 5 visualizes the decreased metallobasicity of gold, with the electron density remaining localized on the phenyl ligand and the NPA charge of Au significantly increasing from 0.23 to 0.43. Computational spectroscopic parameters further emphasize this change with an increased OH stretching frequency and an upfield shift of the OH peak in the ^{1}H NMR spectrum.

In summary, by exchanging chloride for a more electron-donating phenyl ligand, we were able to increase the metallobasicity of Au, thereby augmenting an intramolecular Au···H-O HB. This HB was verified experimentally through SCXRD as well as NMR and IR spectroscopy. An array of computations further validated this interaction, and significant differences were noted between the phenylated and chlorinated systems.

This work was performed at Texas A&M University with support of the National Science Foundation (CHE-2154972), the Welch Foundation (A-1423), and Texas A&M University (Arthur E. Martell Chair of Chemistry). We thank Dr. Nattamai Bhuvanesh for his advice regarding the crystallography.

Conflicts of interest

There are no conflicts to declare.

Notes and references

1. A. Martín, *J. Chem. Educ.*, 1999, **76**, 578.
2. E. Arunan, G. R. Desiraju, R. A. Klein, J. Sadlej, S. Scheiner, I. Alkorta, D. C. Clary, R. H. Crabtree, J. J. Dannenberg, P. Hobza, H. G. Kjaergaard, A. C. Legon, B. Mennucci and D. J. Nesbitt, *Pure Appl. Chem.*, 2011, **83**, 1619-1636.
3. E. Arunan, G. R. Desiraju, R. A. Klein, J. Sadlej, S. Scheiner, I. Alkorta, D. C. Clary, R. H. Crabtree, J. J. Dannenberg, P. Hobza, H. G. Kjaergaard, A. C. Legon, B. Mennucci and D. J. Nesbitt, *Pure Appl. Chem.*, 2011, **83**, 1637-1641.
4. L. Brammer, *Dalton Trans.*, 2003, 3145-3157.
5. A. Albinati, C. G. Anklin, F. Ganazzoli, H. Ruegg and P. S. Pregosin, *Inorg. Chem.*, 1987, **26**, 503-508; W. Yao, O. Eisenstein and R. H. Crabtree, *Inorg. Chim. Acta*, 1997, **254**, 105-111; Y. Zhang, J. C. Lewis, R. G. Bergman, J. A. Ellman and E. Oldfield, *Organometallics*, 2006, **25**, 3515-3519.
6. P. Pyykkö and J. P. Desclaux, *Acc. Chem. Res.*, 1979, **12**, 276-281.
7. M. Baya, Ú. Belío and A. Martín, *Inorg. Chem.*, 2014, **53**, 189-200.
8. R. J. Berger, J. Schoiber and U. Monkowius, *Inorg. Chem.*, 2017, **56**, 956-961.
9. J. M. López-de-Luzuriaga, A. Sladek and H. Schmidbaur, *J. Chem. Soc., Dalton Trans.*, 1996, 4511-4512; H. Schmidbaur, H. G. Raubenheimer and L. Dobrzańska, *Chem. Soc. Rev.*, 2014, **43**, 345-380.
10. M. Kumar and J. S. Francisco, *J. Am. Chem. Soc.*, 2020, **142**, 6001-6006.
11. X. Lin and Y. Mo, *Inorg. Chem.*, 2021, **60**, 460-467.
12. F. Groenewald, J. Dillen, H. G. Raubenheimer and C. Esterhuysen, *Angew. Chem. Int. Ed.*, 2016, **55**, 1694-1698.
13. F. Groenewald, H. G. Raubenheimer, J. Dillen and C. Esterhuysen, *Dalton Trans.*, 2017, **46**, 4960-4967.
14. F. Groenewald, H. G. Raubenheimer, J. Dillen and C. Esterhuysen, *J. Mol. Model.*, 2019, **25**, 135.
15. M. Straka, E. Andris, J. Vícha, A. Růžička, J. Roithová and L. Rulíšek, *Angew. Chem. Int. Ed.*, 2019, **58**, 2011-2016.
16. M. Rigoulet, S. Massou, E. D. Sosa Carrizo, S. Mallet-Ladeira, A. Amgoune, K. Miqueu and D. Bourissou, *Proc. Natl. Acad. Sci. U.S.A.*, 2019, **116**, 46.
17. G. Park and F. P. Gabbaï, *J. Am. Chem. Soc.*, 2021, **143**, 12494-12498.
18. K. Chansaenpak, M. Yang and F. P. Gabbaï, *Phil. Trans. R. Soc. A*, 2017, **375**, 20170007.
19. J. Coates, in *Encyclopedia of Analytical Chemistry*, 2000, vol. 12, pp. 10815-10837.
20. T. Maekawa, H. Sekizawa and K. Itami, *Angew. Chem. Int. Ed.*, 2011, **50**, 7022-7026.
21. A. Bondi, *J. Phys. Chem.*, 1964, **68**, 441-451.
22. N. V. Tzouras, M. Saab, W. Janssens, T. Cauwenbergh, K. Van Hecke, F. Nahra and S. P. Nolan, *Chem. Eur. J.*, 2020, **26**, 5541-5551.
23. M. R. Churchill, *Inorg. Chem.*, 1973, **12**, 1213-1214; M. Lusi and L. J. Barbour, *Crystal Growth & Design*, 2011, **11**, 5515-5521.
24. S. Emamian, T. Lu, H. Kruse and H. Emamian, *J. Comput. Chem.*, 2019, **40**, 2868-2881; P. Kolandaivel and V. Nirmala, *J. Mol. Struct.*, 2004, **694**, 33-38.

